Microsructural Analysis of Zinc-Clay Cermet Resistors

O.A. Babalola*, A.B. Alabi and T. Akomolafe.
Physics Department, University of Ilorin, Nigeria.
babalolaOA@gmail.com

Abstract: Cermet rods of dimensions of 65mm × 6.5 mm × 3.2 mm were produced by a mould using a compaction method with a pressure of $(6.35 \pm 0.02) \times 10^8$ N/m^2. The cermets were produced with zinc powder content of 10 % and 70 % (vol.). The rods were subjected to varying annealing temperatures ranging from 300 ^{o}C to 1000 ^{o}C using an electric furnace for a time duration of one hour. Microstructural changes due to cermets composition and annealing temperatures were done using x-ray diffraction (XRD), x-ray fluorescence (XRF), scanning electron microscopy (SEM) and optical micrographs. The changes in physical structures and chemical compositions responsible for the changes observed in electrical resistivity of the cermets were also investigated. [Researcher. 2010; 2(3):48-55]. (ISSN: 1553-9865).

Keywords: Cermet; Microstructure; Clay; Resistors

1.0 Introduction

Ceramics comprise of crystallites that may vary in structure, perfection and composition as well as in size, shape and internal stresses to which they are subjected (Zhang et al, 2003). In addition, the interfaces between crystallites are the regions in which changes in lattice orientation occur, often accompanied by differences in composition and attendant electrical effects. As a consequence, it is very difficult, if not impossible, to account precisely for the electrical behaviour of ceramics.

The study of single-crystal properties of principal components has resulted in valuable insights into the behaviour of ceramics. However, the growth of single crystals is usually a difficult and time-consuming (Ram et al, 2001). The complexities of ceramic microstructures render the prediction of properties of the ceramic uncertain unlike those of the corresponding single crystals.

When mixtures of ceramic and metal powder is put under suitable pressure followed by sintering, the resultant is known as cermet. Cermets produced from materials such as Co:Al_2O_3 (Ram et al, 2001), molybdenum-zirconia (Coral et al, 1999), Ruthenate(Prudenziati, 1993; Morten et al,1994) and metal-clay(Akomolafe and Oladipo,1996; Ayodele and Akomolafe, 2005) among others have been reported.

Distinctive band structure type exists for each of the metals, semiconductors and insulators. An electron becomes free by being excited from a filled state in one band, to an available empty state above the Fermi energy. Relatively small energies are required for electron excitations in metals, giving rise to large number of free electrons being produced. Larger energies are required for electron excitations in semiconductors and insulators which is responsible for their lower free electron concentrations and smaller conductivity values (Wieczorek-Ciurowa et al, 2008; Callister, 1997; Ayodele and Akomolafe, 2005).

Free electrons that are acted on by an electric field get scattered by imperfections in the crystal lattice. The magnitude of electron mobility is indicative of the frequency of these scattering events. In many materials, the electrical conductivity is proportional to the product of the electron concentration and mobility (Abdel-Wahab; 2004). For metallic materials, electrical resistivity increases with temperature, impurity content, and the amount of plastic deformation. The contribution of each of these to the total resistivity is additive (Callister, 1997).

Material science study involves investigating the relationships that exist between the structures and properties of materials. Virtually all the important properties of solid materials may be grouped into six different categories namely, mechanical, electrical, thermal, magnetic, optical and deteriorative (ageing) (Callister, 1997). Electrical properties relate to properties such as electrical conductivity, and dielectric constant that are stimulated by an electric field.

Thick-Film resistors (TFR) are a special class of cermet materials that show relevance role in microelectronics (Prudenziati, 1993). The conduction mechanisms consistent with their microstructure have been studied by several researchers (Prudenziati, 1993; Ayodele and Akomolafe, 2005; Morten et al, 1994; Aghamalyan et al, 2003). The electrical properties analysed include different possibilities such as hopping of electrons from and to conductive grains and localized states in the glassy matrix. Also, direct tunnelling of electrons between near-neighbouring grains assisted by resonant centres in the intergranular material and conduction in a narrow band of nearly delocalized states in the intergranular material (Prudenziati, 1993). Deep energy levels in the glass

seem to play significant roles in the conduction mechanisms of TFRs .

2.0 Material and Methods:

It is known that changes in electrical properties of cermets are associated with physical, mechanical, thermal and chemical changes within its structure(Akomolafe and Oladipo, 1996). This work is thus aimed at describing the microstructural changes, which affect the electrical properties such as resistivity, TCR, VDR, size-effect and variation of these properties with annealing schedule, concentration of the conductive phase, etc. of zinc-clay cermets.

The two most important independent variables in use for this research work are: The relative concentration of zinc powder with respect to clay powder and the initial firing temperature otherwise known as the annealing temperature. Other variables are annealing time, the cermet temperature and applied potential difference.

The microstructural analyses of the zinc-clay cermets are done using scanning electron microscope and photomicroscope at various zinc concentrations and annealing temperatures while the chemical analyses was done using X-ray fluorescence (XRD).

The effects of annealing schedule (peak firing temperature and annealing time), the cermets composition, (zinc-clay ratio and particle size) and microstructural changes on the electrical properties of zinc-clay cermets have also been investigated.

Cermet rods of dimensions of 65mm × 6.5 mm × 3.2 mm were produced by a mould using a compaction method with a pressure of $(6.35 \pm 0.02) \times 10^8$ N/m^2. The cermets were produced with zinc powder content of 10 % and 70 % (vol.). The rods were subjected to varying annealing temperatures ranging from 300 ^{o}C and 1000 ^{o}C using an electric furnace for a time duration of one hour.

2.1 Scanning Electron Microscopy (SEM):

The *Stereoscan 430i* scanning electron microscope at Universita Degli Studi Trieste, Italy was used to obtain the micrographs of the resistors. Five resistors, which contain 10 %(vol.) Zn-clay ratio and another five resistors containing 70 %(vol.) Zn-clay ratio were produced, representing cermets with zinc filler above and below the cermets percolation threshold. Each cermet was annealed at 300 ^{o}C, 500 ^{o}C, 700 ^{o}C and 1000 ^{o}C and thereafter the photomicrographs were taken. Table 1 shows the samples and their annealing temperatures.

Sample	Zn Filler concentration % (vol)	Annealing Temperature ^{o}C
A	70	1000
B	70	700
C	70	500
D	70	300
E	70	Un-annealed
F	10	1000
G	10	700
H	10	500
I	10	300
J	10	Un-annealed

Table 1. Samples selected for scanning electron micrographs.

Pictures were taken of each of the samples using four different magnifications of x100, x200 and x500 and x1000 at 15.00 kV potential.

2.2 Optical Photomicrographs

Each of the sample i.e. A to J as seen in Table 1 was presented for optical photomicrographs at a magnification of x 750.

2.3 X-ray Fluorescence (XRF):

X-ray fluorescence study was done and recorded for each of the samples A - J to study the energy transitions in the inner-shell electrons. The machine used is the Link Analytical (ISIS) situated at the University of Trieste, Italy with maximum beam energy of 25 keV.

2.4 X-ray Diffraction (XRD):

In order to determine the crystalline structure of the pure clay powder which has been annealed for duration of 60 minutes at 1000 ^{o}C, the XRD of clay powder was taken at angles between 5^o and 80^o in steps of 0.02^o. The step time is 5 seconds/step and the step size is 0.02. The x-ray diffraction of the pure clay was done so as to compare the structure of the pure clay crystal formed with the structure of the cermets after both have been annealed at 1000 ^{o}C.

All the cermets were fired in the Vecstar furnace at the required annealing temperature for a time duration of 60 minutes. Thereafter, the cermets were allowed to cool slowly in the oven.

3.0 Results and Discussion

The microstructure of the zinc-clay cermet reveals a lot about the internal structure of the cermet and how they affect its electrical properties. The XRD, XRF, SEM and the optical microscope examination were used in performing the microstructural analyses of the cermets.

3.1 X-ray Diffraction:

The x-ray diffraction of 100 % (vol.) clay powder which has been fired for a time duration of one hour at 1000 ^{o}C was performed to determine if the structure of the clay powder become crystalline or amorphous after annealing. It is known that scattering of an x-ray beam by a crystal will give rise to a large number of diffraction maxima, the position of which are related to the lattice parameter, the miller indices and the x-ray wavelength (Weller, 1994).

Fig 1 shows the x-ray diffraction pattern for 100 %(vol.) clay powder fired at 1000 ^{o}C. The diffraction pattern suggests that clay fired at this temperature has a high level of amorphous phase since the background noise in the diffraction pattern is high (Weller, 1994). However, three peaks were observed at 20.7^{o}, 63.0^{o} and 26.4^{o}. The peak observed at 26.4^{o} was as a result of the aluminium sample holder that unfortunately interfered with the x-ray beam. However, the strong peaks seen at 20.7^{o} and 63.0^{o} suggest that the fired clay also contains a few crystalline phases.

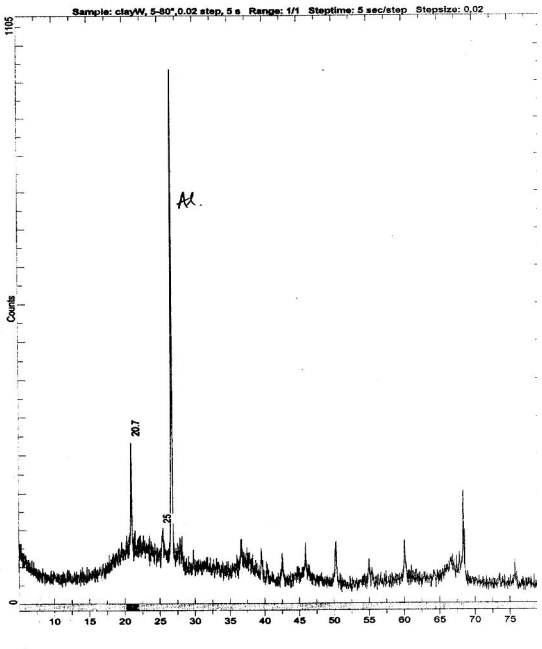

Fig. 1. X-Ray Diffraction for 100% (vol.) Clay Powder fired at 1000 ^{o}C

X-Ray Fluorescence:

X-ray fluorescence for 10 %(vol.) and 70 %(vol.) zinc-clay cermets annealed at 300 ^{o}C, 500 ^{o}C, 700 ^{o}C and 1000 ^{o}C were performed to ascertain the relative concentration of the various elements making up the cermets in relation to the zinc concentration and annealing temperature. The x-ray fluorescence was also done for the un-annealed sample.

Figure 2a shows the x-ray fluorescence of the un-annealed 10% (vol.) zinc composition resistors while Figures 2b and 2c are the x-ray fluorescence of the same zinc concentration but annealed at 500 ^{o}C and 1000 ^{o}C. Also, Figure 3a show the x-ray fluorescence of the un-annealed 70% (vol.) zinc composition resistors while Figures 3b and 3c are the x-ray fluorescence of the same composition also annealed at 500 ^{o}C and 1000 ^{o}C. It can be seen that the major elements, which make up the cermet include silicon, aluminium, zinc, oxygen and gold. Other minor constituents include potassium, calcium, iron, magnesium and titanium. These metallic impurities may therefore increase slightly the electrical conductivity of the cermets at low (v_f < 10 %(vol.)), zinc filler contents.

From Figure 2, we show for composites containing 10 %(vol.) that the oxygen content of the cermet increases only slightly with increasing annealing temperatures.

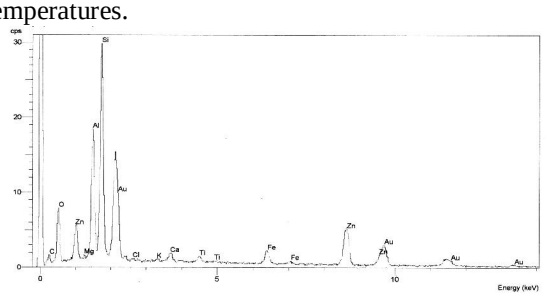

(a.) Un-annealed

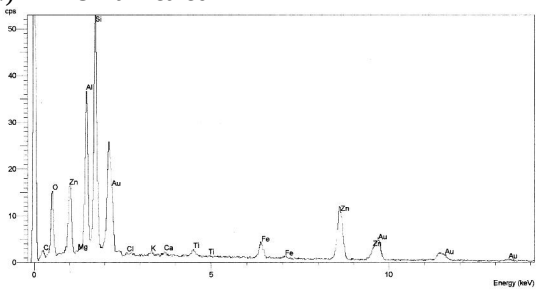

(b.) Annealed at 500 ^{o}C

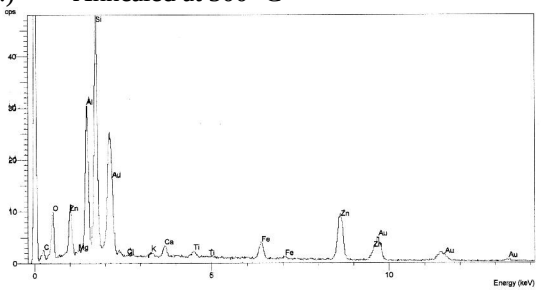

(c.) Annealed at 1000 ^{o}C

Fig. 2. X-ray Fluorescence for 10%(vol.) Zn-clay Cermets (a.) un-annealed, (b.) Annealed at 500 ^{o}C and (c.) Annealed at 1000 ^{o}C

This suggests that oxidation from the furnace atmosphere plays a minor role in the microstructural composition of the zinc-clay cermet with increasing annealing temperatures. This is also confirmed in Fig. 3, which show the x-ray fluorescence for 70 %(vol.) Zn-clay composite.

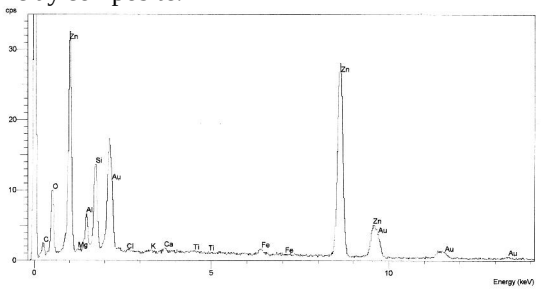

(a.) Un-annealed

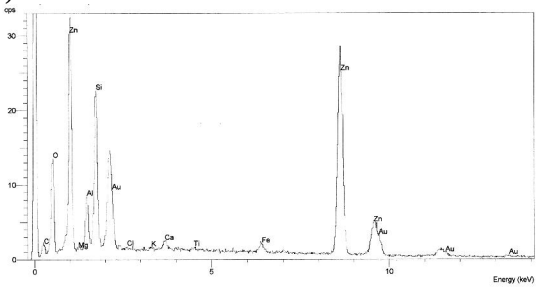

(b.) Annealed at 500 ^{o}C

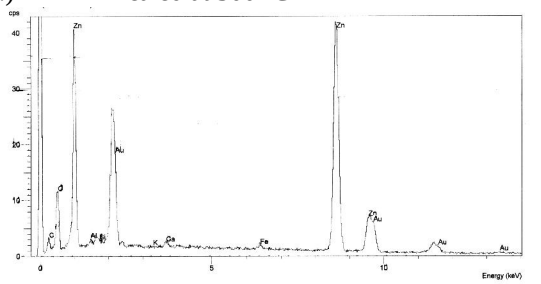

(c.) Annealed at 1000 ^{o}C

Fig. 3. X-ray Fluorescence for 70%(vol.) Zn-clay Cermets (a.) un-annealed, (b.) Annealed at 500 ^{o}C and (c.) Annealed at 1000 ^{o}C

Diffusion of oxygen into the cermet is low probably because of its low porosity caused by close compaction of cermet powders with a large compressive force in the order of $(6.35\pm0.02)x10^{8}$ N/m^{2}. The increase in cermets resistivity noticed in cermets annealed at temperatures greater than 700 ^{o}C may therefore not be as a result of direct oxidation but due to depletion through formation of zinc complexes with the clay compound.

Scanning Electron Microscopy:

Figures 4 and 5 show the micrographs for the samples of zinc-clay cermets containing 10 % (vol.) zinc annealed at 300 ^{o}C, 500 ^{o}C, 700 ^{o}C and 1000 ^{o}C respectively.

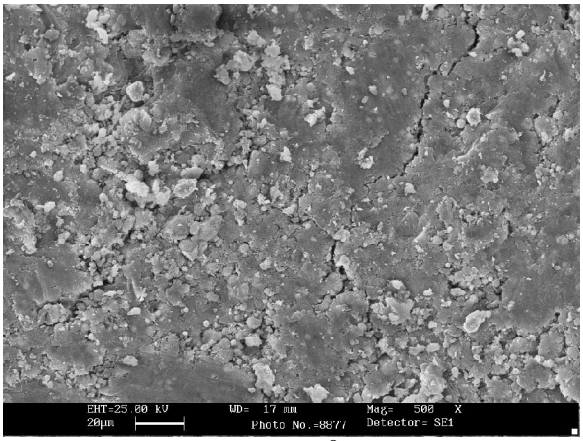

(a.) Annealed at 300 ^{o}C

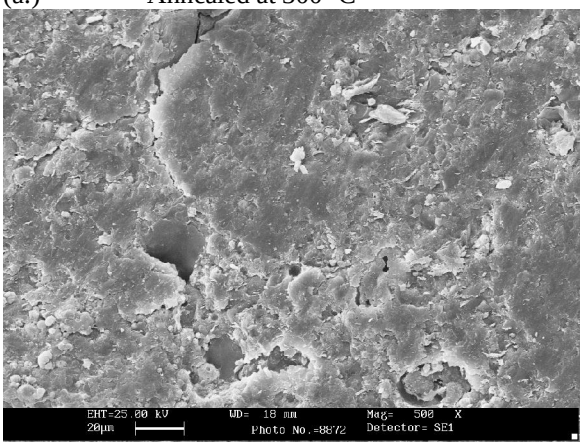

(b.) Annealed at 500 ^{o}C

Fig. 4. SEM micrographs of zinc-clay cermet containing 10% (vol.) Zn Viewed at a magnification of 500x (a.) annealed at 300 ^{o}C (b.) annealed at 500 ^{o}C

Figures 6 and 7 also show the micrographs of zinc-clay cermet composition containing 70% (vol.) zinc annealed at the same annealing temperatures of 300 ^{o}C, 500 ^{o}C, 700 ^{o}C and 1000 ^{o}C respectively.

Evidences of micro-cracks were present in the cermet annealed at temperatures below and equal to 500 ^{o}C as seen in Figs. 4 and 6. It is observed here that the magnitude and density of the cracks reduces with increasing annealing temperatures. This may be responsible for the relatively high resistivity of cermets annealed below 500 ^{o}C as seen in Figure 11, which show the variation of cermets resistance with annealing temperature. Also at these temperatures ($T_f \leq 500$ ^{o}C) the grain structure of the cermets is very pronounced.

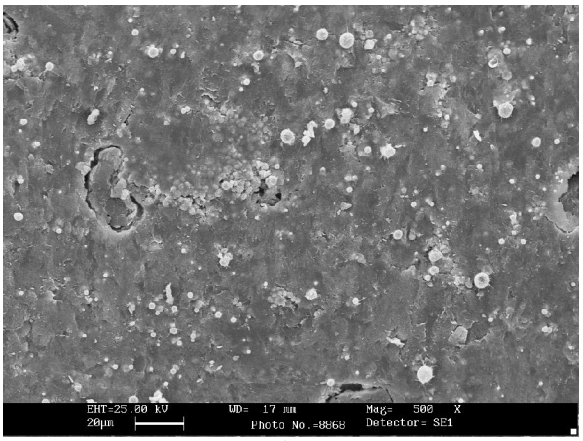

(a.) Annealed at 700 ^{o}C

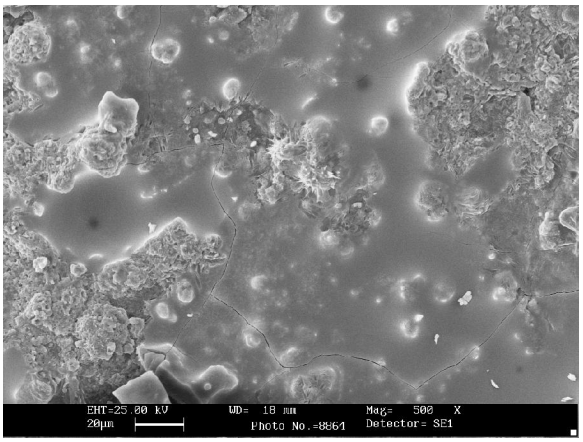

(b.) Annealed at 1000 ^{o}C

Fig. 5. SEM micrographs of zinc-clay cermet containing 10% (vol.) Zn Viewed at a magnification of x 500 (a.) annealed at 700 ^{o}C (b.) annealed at 1000 ^{o}C

The pronounced grain structure is probably the cause of the strong voltage dependences of resistance noticed for cermets fired at these range of annealing temperatures as seen in figure 8.

A marked transition in cermets morphology in seen to occur for cermets annealed at 500 ^{o}C as seen in Figs. 4b and 6b. At low filler concentration of 10 % (vol.) Zn, it can be seen that the micro-cracks within the cermets have given way to a sheet-like structure while at high filler concentration of about 70 % (vol.) Zn, apart from the glassy part of the structure, a fibre-like growth is found on the surface.

There is not much significant difference in the microstructure of the cermets annealed at temperatures below 500 ^{o}C . This may then suggest the reason why annealing below 400 ^{o}C does not significantly influence the electrical properties of the un-annealed zinc-clay composites. The result of lack of sintering at these annealing temperatures is most likely the cause of the high electrical resistance, low mobility and high TCR observed. The SEM micrographs show the presence of micro-cracks and show that oxides and fluxes from the clay may coat the zinc grains. The average zinc particle size (diameter) was found to be about 3.5 µm at T_f = 300 ^{o}C.

Figure 6 shows some needle-like growth emerging from the zinc-clay cermet structure. These needle-like growths are pronounced at higher zinc concentrations showing that they are products from zinc rather than clay. Their crystalline shapes suggest that they were formed during the slow cooling of the cermets after firing at the required temperature.

These needle-like growths increase in size and number when the annealing temperature increases from 300 to 700 ^{o}C (Figs. 6 and 7). The longest length (Fig 7) is about 45 µm long and about 2 µm thick. The average length and thickness is however about 10 µm long and 0.5 µm thick.

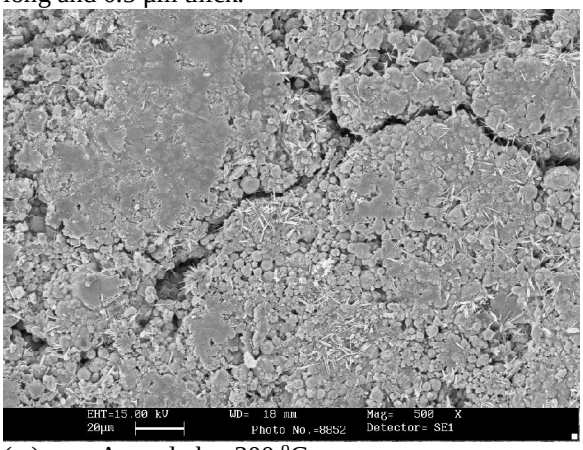

(a.) Annealed at 300 ^{o}C

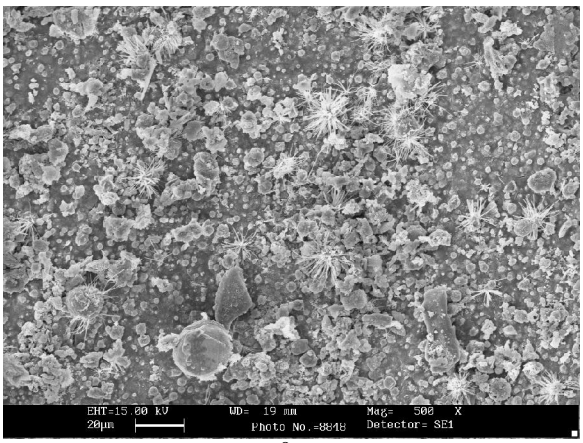

(b.) Annealed at 500 ^{o}C

Fig. 6. SEM micrographs of zinc-clay cermet containing 70% (vol.) Zn Viewed at a magnification of 500x (a.) annealed at 300 ^{o}C (b.) annealed at 500 ^{o}C

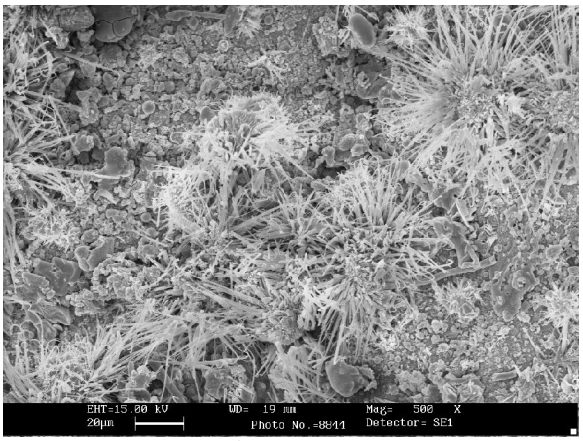

(a.) Annealed at 700 ^{o}C

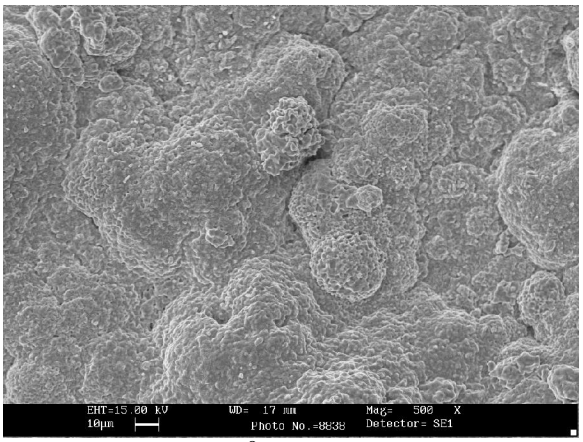

(b.) Annealed at 1000 ^{o}C

Fig. 7. SEM micrographs of zinc-clay cermet containing 70% (vol.) Zn Viewed at a magnification of 500x (a.) annealed at 700 ^{o}C (b.) annealed at 1000 ^{o}C

Annealing the cermets at 1000 ^{o}C totally changes the morphology of the cermets. All the grain growth and crystalline phases give way to a glassy surface (Fig 5b.) at low filler concentration and to an amorphous phase at high concentration (Fig 7b). This sudden change in morphology is most likely the cause of the extremely high resistance observed for all the resistors annealed at 1000 ^{o}C. It is expected at this temperature that all free zinc metals have been oxidized or combined chemically with other elements or compounds within the cermet structure. There is also the possibility of vaporization of the zinc metal but the XRF in figure 3 suggests otherwise since it shows no marked reduction in zinc content with increasing annealing temperatures. The boiling point of zinc is 907 ^{o}C thus chemical reaction of all the free zinc metal must have occurred well before its boiling point.

It is suggested that the fibre-like growth aid conduction and are responsible for the switching effects observed as the annealing temperature range between 500 ^{o}C and 700 ^{o}C.

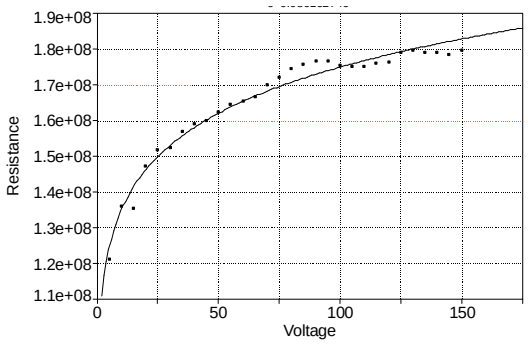

Fig. 8 Variation of Cermet Resistance with applied p.d for 25%(vol.) Zn filler concentration (T_f = 300 ^{o}C)

Optical Micrographs:

Optical micrographs of the cermets with zinc concentrations of 10 and 70 % (vol.) were taken at a magnification of x850 for both the annealed and un-annealed samples.

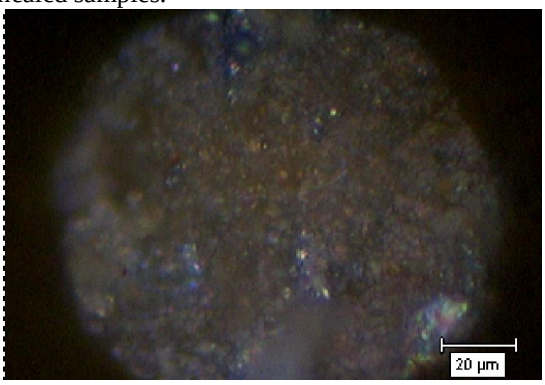

(a.) Photomicrographs of Zn-clay Cermets containing 10%(vol.) Zn

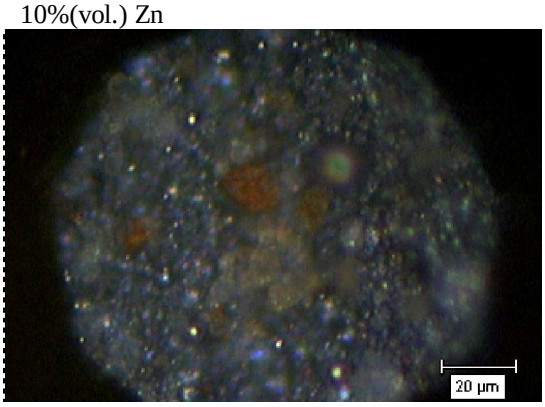

(b.) Photomicrographs of Zn-clay Cermets containing 70%(vol.) Zn

Fig. 9 Photomicrographs of Zn-clay Cermets containing 10 % and 70%(vol.) Zinc , annealed at 700 ^{o}C

Fig 9 shows the photomicrographs of Zn-clay cermets containing 10 % and 70 %(vol.) Zinc, annealed at 700 ^{o}C, which shows spots of shining globules, which are free zinc metal. The spherical nature suggests that cohesion of zinc (powder) particles occurred after the zinc metal powder in the cermet structure has melted.

Figure 10 shows the photomicrograph of the cermet annealed at 1000 ^{o}C. It shows the absence of the free zinc metals in the structure and showing instead rowdy patches, which is an evidence that major chemical interaction have occurred between the free zinc metal and the clay substrate.

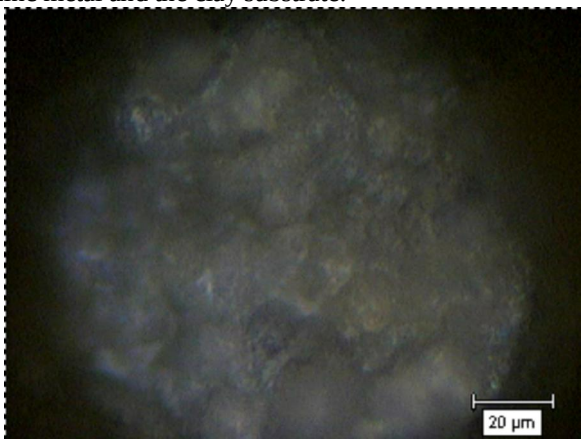

Fig.10 Photomicrographs of Zn-clay Cermets containing 70%(vol.) Zinc annealed at 1000 ^{o}C

The dark nature of the micrograph indicates complete elimination of the free zinc metals and this account for the high resistance recorded for the samples annealed at this temperature.

Figure 11 shows the variation of cermet resistance with annealing temperatures. At low annealing temperatures (Fig. 11a), cermet resistance reduced with increasing annealing temperature. The initial high resistance when T_f=300 ^{o}C was most likely the result of micro-cracks existing at low annealing temperatures (Fig. 6.) which is due to incomplete sintering of the cermet structure. The cermet resistance decreased with increasing annealing temperature until T_f is approximately 600 ^{o}C. This is as a result of improved sintering of the cermet structure with annealing temperatures. Above 700 ^{o}C however, (Fig. 11b.) an exponential increase in resistance was observed.

This behaviour is consistent with decrease in free zinc metal within the cermet structure as discussed with Fig. 7b.

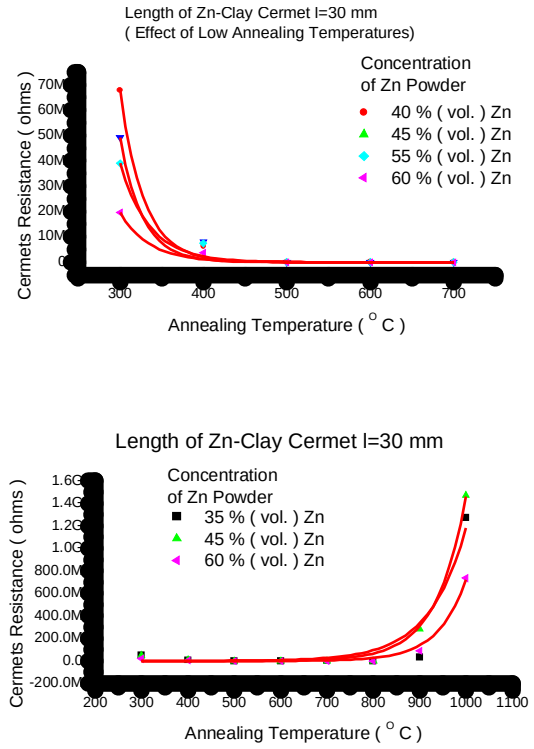

Fig. 11 Variation of Cermets Resistance with Annealing Temperature for 35 -60% (vol.) Zn- Clay ratio.

4.0 Conclusion:

The microstructural analyses of the cermets at various composition and annealing temperatures were carried out for more understanding of the electrical properties of the cermet. This is because, the microstructure of the zinc-clay cermet reveals a lot about the internal structure of the cermet and how they affect its electrical properties. The XRD, XRF, SEM and the optical microscope have been used in performing the microstructural analyses of the zinc-clay cermets with respect to variation of its electrical resistivity with zinc content and annealing temperatures.

It was found from this work that changes in electrical properties of cermets are associated with physical, mechanical and chemical changes within its structure. This is responsible for the strong dependence of cermets resistance on applied voltage occurring due to large number of inter-grain boundaries existing at low annealing temperatures $T_f \leq 400$ ^{o}C. High cermet resistivity at annealing temperatures less than 400 ^{o}C has been shown to be the result of micro-cracks existing at these annealing temperatures due to incomplete sintering. The increased resistivity of the cermets as the annealing temperature exceeds 700 ^{o}C has also been shown to be associated with depletion of free zinc metal within the cermet structure due to chemical reaction of zinc to form complexes with the clay ions.

References:

1. Abdel-wahab, F.: The normal and inverted Meyer-neledel rule in the ac conductivity. Turk. J. Phys. 28,133-138(2004).
2. Aghamalyan, N.R., Gambaryan, I.A., Goulanian, E.K., Hovsepyan, R.K, Kostanyan,R.B., Petrosyan, S.I., Vardanyan,E.S. and Zerrouk, A.F: Influence of thermal annealing on optical and Electrical Properties of ZnO films by electron beam evaporation. Semicond. Sci. Technol. 18, 525-529.(2003).
3. Akomolafe, T., Oladipo, O.: Electrical Properties of Fe-Clay Composite Resistors. Material Letters. 27, 145-153(1996).
4. Ayodele, S. , Akomolafe, T. : DC Electrical Properties and Conduction Mechanisms of Al-Clay based Composite Resistors. Journal of Material Science. 40, 6131-6138 (2005).
5. Callister William D: Material Science and Engineering: An Introduction. Wiley. 6th Edition. (1997).
6. Coral M. Lukaniuk, Lorne D. Schwartz, Thomas H. Etsell: A new method for the production of a molybdenum-zirconia cermet. Journal of Material Research. 14, 1801-1804 (1999).
7. Morten, B., Masoero, A., Prudenziati, M., Manfredini, T. : Evolution of Ruthenate-Based thick Film Cermet Resistors. Journal of Physics D: Applied Physics. 27, 2227-2235 (1994).
8. Nielson F.P. Ribeiro, Mariana M.V.M Souza, Octavio R. Macedo Neto, Sonia M.R. Vasconcelos, Martin Schmal : Investigation of Ni/YSZ cermet as Anode for SOFC applicationas. Applied Catalysis A: General. 353, 305-309(2009).
9. Prudenziati, M.: Electrical Transport in Thick Film (Cermet) Resistors. Electrocomponent Science and Technology. 10, 285-293 (1993).
10. Ram, S., Gosh, D., Roy, S.K.: Microstructure and topological Analysis of Co:Al_2O_3 nanocermets in new FCC and BCC Metastable co-structures. Journal of Material Science. 36, 3745-3753(2001).
11. Weller, M.T.: Inorganic material Chemistry. Oxford Chemistry primer. Oxford Science publication.(1994).
12. Wieczorek-Ciurowa, K. , Oleszak, D. , K. Gamrat: Cu-Al/Al_2O_3 Cermet Synthesized by Reactive Ball Milling of CuO-Al system. Reviews on Advanced materials Science. 18, 248-252 (2008).
13. Zhang, W., Sui, M.L., Zhou, Y.Z., Guo, J.D., He, G.H. , Li, D.X.: Evolution of microstructure in TiC/NiCr cermet induced by electropulsing. Journal of Material Research. 18, 1543-1550 (2003).

3/1/2010